

# High-Resolution Mass Spectrometers

Alan G. Marshall[1,2] and Christopher L. Hendrickson[1,2]

[1]National High Magnetic Field Laboratory, Florida State University, Tallahassee, Florida 32310; email: marshall@magnet.fsu.edu; hendrick@magnet.fsu.edu

[2]Department of Chemistry and Biochemistry, Florida State University, Tallahassee, Florida 32306

Annu. Rev. Anal. Chem. 2008. 1:579–99

First published online as a Review in Advance on March 14, 2008

The *Annual Review of Analytical Chemistry* is online at anchem.annualreviews.org

This article's doi: 10.1146/annurev.anchem.1.031207.112945



1936-1327/08/0719-0579$20.00

## Key Words

orbitrap, FTMS, reflectron TOF, Fourier transform, ion cyclotron resonance, FT-ICR

## Abstract

Over the past decade, mass spectrometry has been revolutionized by access to instruments of increasingly high mass-resolving power. For small molecules up to ~400 Da (e.g., drugs, metabolites, and various natural organic mixtures ranging from foods to petroleum), it is possible to determine elemental compositions ($C_cH_hN_nO_oS_sP_p\ldots$) of thousands of chemical components simultaneously from accurate mass measurements (the same can be done up to 1000 Da if additional information is included). At higher mass, it becomes possible to identify proteins (including posttranslational modifications) from proteolytic peptides, as well as lipids, glycoconjugates, and other biological components. At even higher mass (~100,000 Da or higher), it is possible to characterize posttranslational modifications of intact proteins and to map the binding surfaces of large biomolecule complexes. Here we review the principles and techniques of the highest-resolution analytical mass spectrometers (time-of-flight and Fourier transform ion cyclotron resonance and orbitrap mass analyzers) and describe some representative high-resolution applications.

## 1. INTRODUCTION

**Mass-resolving power:** $m/\Delta m_{50\%}$, in which $\Delta m_{50\%}$ is the mass spectral peak full-width at half-maximum peak height

**TOF:** time-of-flight

**FT:** Fourier transform

**MALDI:** matrix-assisted laser desorption/ionization

**ESI:** electrospray ionization

**Mass resolution:** the separation (in Daltons) between two mass spectral peaks (such that the valley between the sum of the peaks is equal to the height of the smaller individual peak)

The history of spectroscopy is the history of resolution. Mass spectrometers typically measure the mass-to-charge ratio ($m/z$) of an ion. As mass-resolving power ($m/\Delta m_{50\%}$, see below) increases, several new plateaus of chemical information become accessible (1):

1. At $m/\Delta m_{50\%} > 100$, there is a separation of different charge states for ions derived from the same neutral analyte [e.g., $(M+H)^+$ versus $(M+2H)^{2+}$, etc.];
2. at $m/\Delta m_{50\%} > 1000$, there is a separation of peaks of different nominal mass (e.g., 325 Da versus 326 Da);
3. at $m/\Delta m_{50\%} > 10{,}000$, the resolution of small (<2500 Da) peptides of the same nominal mass differ by one amino acid (except for isomeric leucine and isoleucine); and
4. at $m/\Delta m_{50\%} > 100{,}000$, there is a separation of peaks for nominally isobaric species (i.e., molecules of the same nominal mass differing in elemental composition, e.g., $N_2$ versus CO, both ~28 Da).

As illustrated below, these capabilities have contributed to the creation of whole new analytical fields ranging from petroleomics to proteomics.

Mass analyzers discriminate among ions of different $m/z$ by subjecting them to constant, pulsed, or periodically time-varying electric and/or magnetic fields (2). This review focuses on the highest-resolution mass analyzers (specifically those capable of routine broadband resolving power >10,000) for analytical chemical and biochemical applications, namely, reflectron time-of-flight (TOF) and Fourier transform (FT) (orbitrap and ion cyclotron resonance) instruments that are compatible with liquid sample introduction and associated ionization techniques [e.g., matrix-assisted laser desorption/ionization (MALDI), electrospray ionization (ESI), and other atmospheric pressure ionization methods]. Other analytical mass analyzers, such as electric/magnetic sectors, quadrupole mass filter, ion trap, triple quadrupole, single-pass TOF, and so on, have important uses but are not optimal for the highest-resolution applications.

### 1.1. Mass Resolution and Mass-Resolving Power

Mass resolution is defined as the minimum mass difference, $m_2 - m_1$, between two mass spectral peaks such that the valley between their sum is a specified fraction of the height of the smaller individual peak. For example, if two equal-magnitude peaks are separated by exactly the width at half-maximum height ($\Delta m_{50\%}$) of either peak (i.e., 50% valley definition; see **Figure 1*a***), then the mass resolution $m_2 - m_1 = \Delta m_{50\%}$. Mass-resolving power may be defined either for a single peak of mass, $m$, as $m/\Delta m_{50\%}$, or for two equal-magnitude peaks as $m_2/(m_2 - m_1)$ (e.g., for 50% valley definition, $m_2/\Delta m_{50\%}$). (For multiply charged ions, $m$ can be replaced by $m/z$ in the above statements.) Mass-resolving power is useful for evaluating mass analyzer performance because it is a measure of precision over a wide range of $m$ (or $m/z$), whereas mass resolution determines the ability to distinguish ions of different

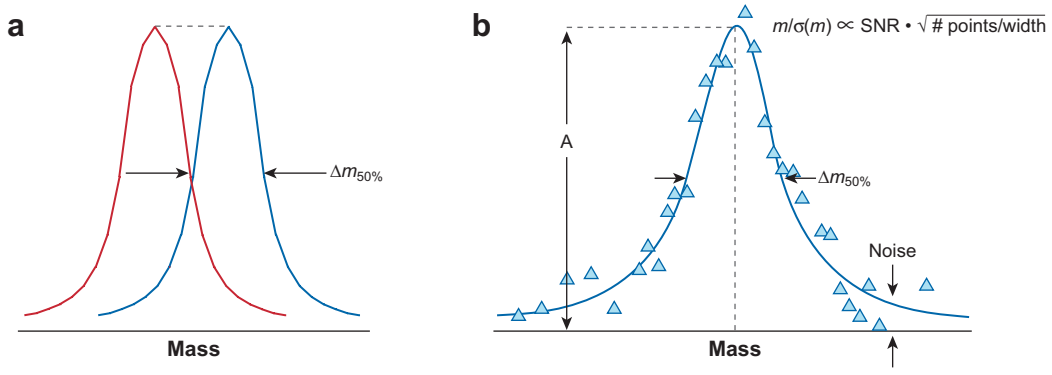


**Figure 1**

(*a*) Two equal-magnitude mass spectral peaks of equal width, separated by one peak width at half-maximum peak height, $\Delta m_{50\%}$. Mass resolution is typically defined as $\Delta m_{50\%}$, whereas mass-resolving power is typically defined as $m/\Delta m_{50\%}$. (*b*) Relation between the mass-measurement precision predicted for the average of many measurements, and the signal-to-noise ratio and number of data points per peak width for a single mass spectrum (see text for details).

elemental composition. For a given mass analyzer, it is important to specify the $m$ (or $m/z$) value at which resolving power or resolution is reported.

## 1.2. Mass-Measurement Precision

Mass imprecision, $\sigma(m)$, may be defined as the root-mean-square deviation of many mass measurements. Conversely, mass precision is $1/\sigma(m)$. However, one would prefer not to have to make many measurements. For an analog (i.e., continuous) mass spectrum, mass precision is simply proportional to the spectral peak signal-to-noise ratio, S/N, for a single measurement. For a discrete mass spectrum (as in most current instruments), mass precision is given by

$$\text{Mass precision} = c\,(\text{S/N})\sqrt{\text{number of data points per peak width}}, \qquad (1)$$

in which $c$ is a constant (of order unity) determined by the peak shape and spectral baseline noise is independent of signal (as in the FT instruments described below) (3). A similar expression applies to ion-counting mass analyzers, except that the peak height imprecision is the square root of the number of counts (4). Thus, it is possible to predict the precision that would be obtained from many measurements on the basis of the S/N and discrete sampling for a single measurement (see **Figure 1*b***).

Equation 1 shows that high mass-measurement precision requires the highest possible S/N and smallest digital point spacing. Thus, mass-measurement precision for low-magnitude peaks (as in many applications) is necessarily lower than for high-magnitude peaks (as typically advertised by mass spectrometer vendors). Equation 1 helps explain why TOF mass analyzer mass-measurement precision has improved

greatly over the past decade, partly from increased resolving power but also from faster digitizers (to give more data points per peak width).

### 1.3. Mass Accuracy and Mass Calibration

Exact molecular mass is calculated from the combined atomic masses (usually based on the most abundant isotope for each atom) of the elemental composition (e.g., $C_cH_hN_nO_oS_sP_p$) of an ion or molecule, for example, 12.000000 + 4(1.007825) = 16.0313 Da for $CH_4$. Note that exact mass of an element differs from the usual "chemical" definition of atomic mass, which is the abundance-weighted average overall isotopes of that element. Mass calibration consists of fitting the observed mass measurements to the accurate masses of two or more different ions. Calibration may be internal (i.e., the reference masses are for ions of known elemental composition in the same mass spectrum as the analyte) or external (i.e., reference masses from a mass spectrum of another analyte acquired under similar conditions). Internal calibration is typically at least twice as accurate as external calibration. The advantages of external and internal calibration may be combined if ions are alternately injected from analyte and reference samples but accumulated together, thereby allowing for real-time adjustment of the relative magnitudes of analyte and calibrant mass spectral peaks (5).

Finally, the above discussion has been limited to random noise. Systematic errors can affect the accuracy of measurements in separate spectra and even between different peaks in the same spectrum, for example, from space-charge effects due to Coulomb repulsion between ions at sufficiently high density. Thus, it is important to eliminate systematic errors, for example, by maintaining the same number of ions in each measurement (6).

## 2. TIME-OF-FLIGHT MASS ANALYZERS

TOF mass analysis is conceptually simple. If ions of the same initial position and velocity can be simultaneously accelerated (by a pulsed direct-current electric field) to a kinetic energy of $zeV$ electron volts, and then allowed to fly freely (i.e., no external electric or magnetic fields) to a detector located $d$ meters away, then ion TOF is related to $m/z$:

$$\mathrm{TOF} = d\sqrt{1/2\,zeV}\sqrt{m/z}. \quad (2)$$

From Equation 1, it is easy to show that TOF mass-resolving power is related to time resolving power by

$$m/\Delta m = 1/2(t/\Delta t). \quad (3)$$

TOF mass analysis is inherently fast and sensitive because all masses are measured simultaneously (i.e., the multiplex advantage). Scanning instruments (for example, sectors and quadrupoles) sequentially focus only one ion mass on the detector while all others are lost.

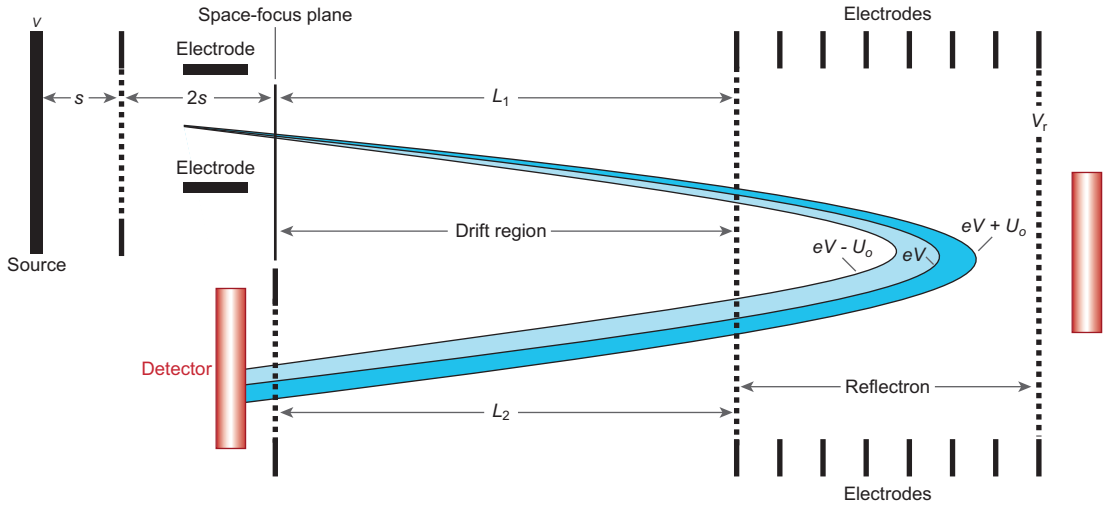


**Figure 2**

Schematic diagram of (*a*) a time-of-flight mass analyzer and (*b*) a reflectron time-of-flight mass analyzer. Figure adapted with permission from Reference 70.

## 2.1. Orthogonal Time-of-Flight Mass Spectrometry

Although it is not possible for different ions to be at the same position and velocity before acceleration, a good approximation is achieved by the orthogonal TOF design, in which a beam of ions (along, say, the *x* axis) is accelerated in a direction (say, the *z* axis) perpendicular to that of the ion beam (7). Thus, ions of different *x*-position and *x*-velocity have essentially the same initial *z*-position before acceleration. Collisional cooling in a radiofrequency multipole ion guide further improves the spatial and velocity distributions (8). TOF resolution can be further improved by tailoring the spatial and temporal accelerating voltage so as to focus ions of the same *m*/*z* but of different initial position and speed at a given postacceleration *z*-position (9).

## 2.2. Reflectron

Additional improvement in TOF resolution is based on an analogy to a mechanical pendulum. To a first approximation, the period of a pendulum is independent of its amplitude of oscillation. Similarly, if ions enter a region of spatially quadratic *z*-potential, then ions of a given *m*/*z* arriving at the same time but with different speed (and thus kinetic energy) will roll uphill until they slow to zero speed, then roll downhill and return to arrive at the detector simultaneously (see **Figure 2**). That reflectron principle (10) thus narrows the TOF distribution for each *m*/*z* and increases the TOF path length, thereby increasing mass-resolving power. Commercial orthogonal reflectron TOF mass analyzers can now routinely attain a

mass-resolving power of >10,000 to yield mass accuracy of ~5–10 ppm if S/N is sufficiently high.

## 2.3. Multiple-Pass Time-of-Flight Mass Spectrometry

In principle, TOF reflectron mass-resolving power should increase by a factor of $n$, for an instrument configured to produce $n$ reflections or energy-isochronous cycles (**Figure 3*a***). In practice, a fraction of the ions is lost at each cycle, and the increase in resolving power with number of reflections is sublinear. Nevertheless, mass-resolving power of 350,000 at $m/z$ 28 ($N_2^+$ versus $CO^+$) has been achieved for 501 cycles of a multiturn electric four-sector TOF instrument (total ion path, 644 m) (11). A second-generation toroidal design eliminates the need for numerous quadrupolar lenses (12).

If ions traverse the same path in each cycle, then the accessible mass spectral $m/z$ range is necessarily reduced by a factor of $n$, so that the mass spectrum is inherently narrowband. Such devices are therefore especially suitable for targeted analysis as might be encountered in outer space and planetary exploration. Extension of the toroids in a third orthogonal direction allows for a spiral rather than planar ion trajectory (**Figure 3*b***) without reduction in $m/z$ range; an eight-turn spiral instrument has demonstrated resolving power of $m/\Delta m_{50\%} = 80{,}000$ at $m/z = 2564$ (the peptide ACTH18–39) (13).

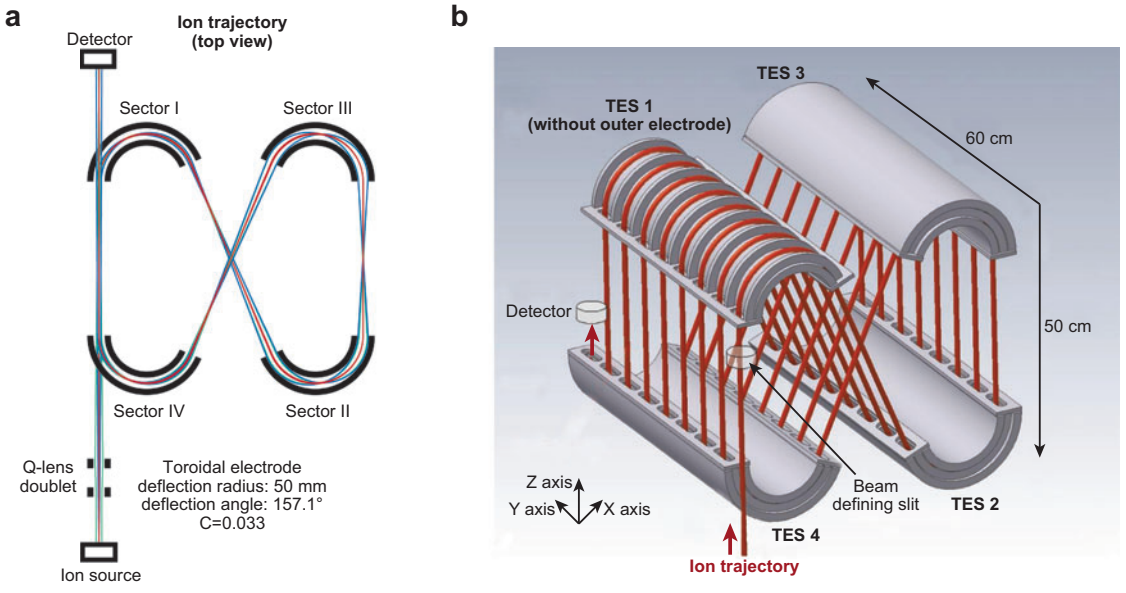


**Figure 3**

Two multiple-pass time-of-flight mass analyzer designs. (*a*) Multum II, with four toroidal sectors. Figure adapted with permission from Reference 71. (*b*) Spiral ion optical device. See text for discussion. Figure adapted with permission from Reference 13.

## 3. FOURIER TRANSFORM MASS ANALYZERS: COMMON FEATURES

### 3.1. Fourier Transform Spectroscopy

**ICR:** ion cyclotron resonance

Ion cyclotron resonance and orbitrap mass analyzers are based on measurements of rf rather than on ion deflection (electric/magnetic sectors), ion stability (quadrupole mass analyzer, quadrupole ion trap), or time of transit (TOF). To first order, ion cyclotron resonance (ICR) and orbitrap frequencies are independent of ion energy, and the induced signal is linearly proportional to ion motional amplitude. For such linear response systems, it is possible to obtain a frequency-domain spectrum by Fourier transformation of the time-domain signal for an initially spatially coherent ion packet. In ICR, initially spatially incoherent ions of a given $m/z$ become spatially coherent following resonant rf electric field excitation; in the orbitrap, spatial coherence is achieved by the injection of ions of a given $m/z$ in a time period that is short in comparison to one cycle of the axial trapping oscillation (see below).

Several common features of FT-ICR and orbitrap MS follow directly from FT data reduction (14). (*a*) Because signals from ions of a wide $m/z$ range can be detected simultaneously, FT MS offers the multiplex advantage of yielding the entire mass spectrum at once, rather than requiring that each peak be scanned through separately. (*b*) Because the magnitude of the response is linearly proportional to the magnitude of the excitation, it is possible to achieve optimally selective and optimally flat-magnitude excitation by specifying its magnitude spectrum and phase-encoding it (usually a quadratic variation of phase with frequency), followed by inverse FT to generate a stored-waveform inverse Fourier transform (SWIFT) time-domain waveform (15, 16). For simple flat-magnitude excitation over a single $m/z$ range, SWIFT reduces to linear frequency sweep excitation (17). Dipolar excitation/ejection in the orbitrap can also be done by SWIFT (18). (*c*) In the zero-collision limit, the time-domain signal is undamped, and FT-MS mass-resolving power varies directly with data acquisition period T (14). However, T is limited in two ways: On-line chromatographic sample introduction limits T to ~1 s, so as to be able to acquire data for several mass spectra during elution of a single chromatographic peak; and the time-domain signal typically decays exponentially with time constant $\tau$. Thus, S/N decreases with time during acquisition, so that T should be no longer than 2–3 $\tau$ (19). (*d*) Digital spectral resolution may be improved by padding an $N$-point time-domain data set with another $N$ zeroes (zero-filling) before discrete FT. However, further zero-fills distort the spectrum without adding new information (20). (*e*) Spectral peak shape may be smoothed by multiplying the time-domain data by any of several apodization waveforms that typically give more weight to the middle time-domain data than to the initial and later data (14). Note that apodization may make the spectra appear better, but actually reduces the information content—a good example of why one should not rely on a visual evaluation of FT spectral data. (For a truncated time-domain signal, apodization can aid in peak-picking, by reducing the Gibbs oscillation "wiggles" on either side of each peak.) In general, any weighting that effectively shortens the time-domain signal must correspondingly broaden the frequency-domain spectral peaks.

### 3.2. Duty Cycle: External Ion Accumulation

Both ICR and orbitrap mass analyzers typically require ~1 s for data acquisition, storage, and processing. However, many of the most useful ionization sources generate ions continuously. Therefore, to not lose ions arriving during mass analysis, it is useful to accumulate ions external to the mass analyzer and then inject them as soon as the preceding data acquisition/processing cycle is complete (in fact the same is true for TOF mass analysis). For ICR, ions are conveniently accumulated in a multipole electric ion trap (21), whereas the orbitrap employs a curved multipole electric ion trap termed the C-trap (22). The next problem is how to eject ions quickly from the external trap, to minimize spatial spreading of ions of a single $m/z$. For ICR, ion ejection may be synchronized by applying 10–30 V to tilted wires placed between the rods of a multipole electric ion trap (23), whereas for the orbitrap, ions are pulsed radially out of the C-trap by a direct-current voltage across two rods and by rapid switching of the rf potential to zero. An advantage of the orbitrap is that the external C-trap may be placed very close to the orbitrap to minimize TOF discrimination.

## 4. FOURIER TRANSFORM ION CYCLOTRON RESONANCE

Ions moving in a spatially uniform static magnetic field, $B$, rotate at a cyclotron frequency, $\nu_c$ (Hz), where

$$\nu_c = ezB/2\pi m, \tag{4}$$

in which $e$ is the elementary charge. At room temperature, typical ion cyclotron orbital radii are at the submillimeter level; moreover, ions of a given $m/z$ rotate with random phase. Thus, to generate a detectable signal, it is necessary to resonantly excite the ions with an oscillating or rotating electric field, to yield a spatially coherent packet of ions of a given $m/z$. The motion of this ion packet gives rise to a time-domain signal consisting of the difference in current induced on a pair of opposed electrodes (see **Figure 4**). This signal is digitized and subjected to discrete fast Fourier transformation to yield a spectrum of ion cyclotron frequencies, which may then be converted to a spectrum of $m/z$.

### 4.1. Mass-Resolving Power

Introduced in 1974 (24), FT-ICR MS has evolved (25, 26) to become the highest-resolution broadband mass analysis technique (27). It is easy to see why. Mass-resolving power in a magnetic sector or TOF mass analyzer depends upon ion path length during the experiment. The highest-resolution double-focusing electric/magnetic sector instrument had an ion path length of ~7 m; a typical TOF instrument has a path length of ~ 1 m, and the multiturn TOF instruments cited above have path lengths ranging from ~20 to 600 m. By comparison, at 9.4 T (a magnetic field equivalent to 400 MHz for proton nuclear magnetic resonance), ions with an $m/z$ of 1000 have a cyclotron frequency of 144,346 Hz and travel $2\pi \times 0.01 \times 144{,}346 = 9070$ meters in one second. Stated another way, FT-ICR resolving power (as defined above) is simply the number of cyclotron orbits during the data acquisition

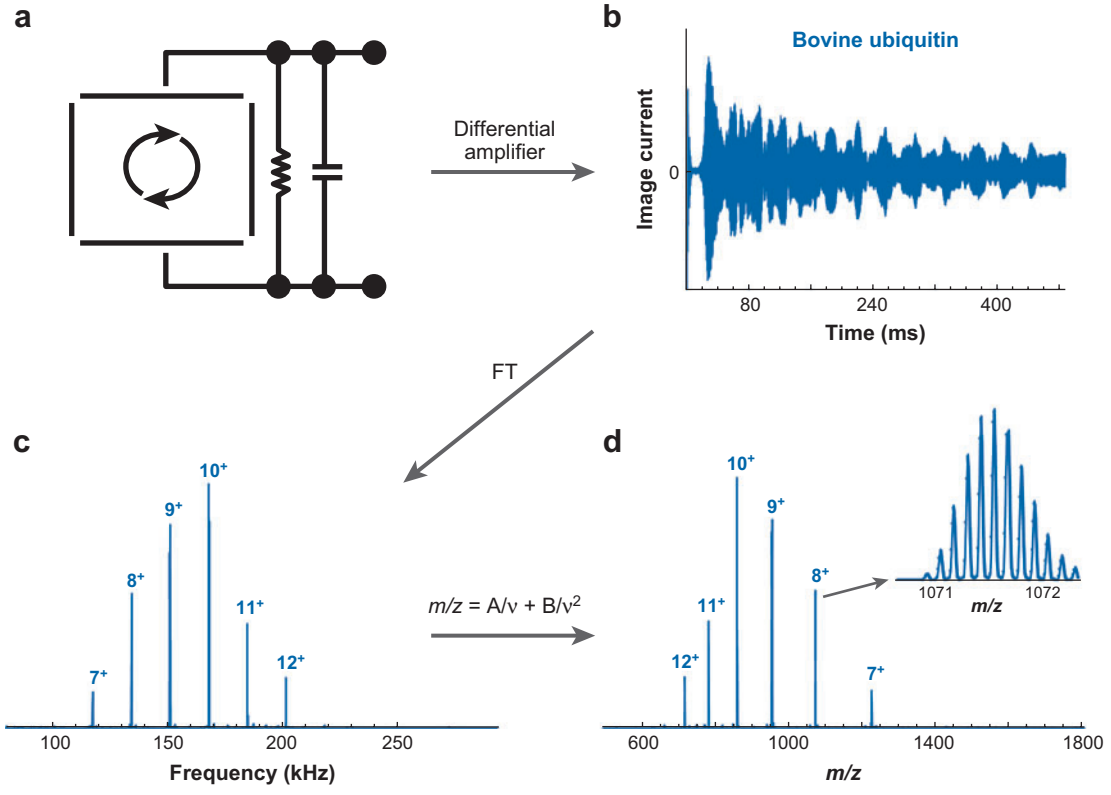


**Figure 4**

(*a*) Schematic representation of excited ion cyclotron rotation, (*b*) time-domain image-current signal from opposed detection electrodes, (*c*) frequency-domain spectrum obtained by fast Fourier transform of the digitized time-domain signal, and (*d*) Fourier transform–ion cyclotron resistance $m/z$ spectrum obtained by calibrated frequency-to-$m/z$ conversion. A full-range mass spectrum (including computation) is typically generated in ~1 s.

period (28): Thus, observation of the same 1000 $m/z$ ions for 3 s yields a potential mass-resolving power of up to $m/\Delta m_{50\%} \approx 400{,}000$. [Even without FT, ion cyclotron frequency detected at liquid helium temperature has achieved single-ion detection and mass accuracy to within better than $10^{-9}$ Da (29), but for low-mass ions and very narrow bandwidth.]

From Equation 4, it is readily shown that ICR mass-resolving power varies as $1/(m/z)$. Moreover, broadband rf excitation and detection electronics are typically flat over approximately a factor of 10 in frequency, and the ion optics that accumulate (21) and transmit ions from the ionization source to the ICR cell in the bore of the magnet also limit the $m/z$ range. Thus, the instrument response is optimally flat over a particular mass range ($200 < m/z < 1000$; $400 < m/z < 2000$, etc.) according to the choice of excitation amplifier, detection preamplifier, and voltage amplitude/frequency applied to ion collection and transmission multipoles.

### 4.2. Nonideal Electric and Magnetic Field Profiles

FT-ICR MS provides much higher resolution and mass accuracy (sub-parts-per-million) than one might expect, given that (*a*) the spatial inhomogeneity of the magnet is 5–20 ppm over the volume of the ICR trap, (*b*) the electrostatic trapping potential is not perfectly quadrupolar, and (*c*) the rf excitation electric field is not spatially uniform. First, the cyclotron rotation of the ions averages out *xy* magnet inhomogeneity, much as for spinning the sample in FT-NMR spectroscopy, and the axial oscillation of ions along the magnetic field averages out magnet axial inhomogeneity. Second, the trapping potential in an ICR cell of virtually any shape (cubic, cylindrical, rectilinear, etc.) approaches quadrupolar near the center of the cell (30); thus, limiting ICR orbital radius to ~1/2 the cell radius reduces nonquadrupolarity. Third, the excitation electric field may be made uniform either by capacitively coupling the end cap and excitation electrodes (31) or by segmenting the end caps (infinity cell) (32).

### 4.3. Magnetic Mirror Effect

The high-field superconducting magnet of an FT-ICR instrument presents a special problem, namely, how to inject externally formed ions through the magnetic field gradient on their way to the ICR cell. The magnetic mirror effect can slow and even reflect off-axis ions of low kinetic energy (33). The solution is to keep the ions focused near-axis by enveloping them in multipole [e.g., quadrupole (34) or octopole (35)] electric ion guides or focusing them along the magnetic field lines with electrostatic lenses (36). The advantage of rf multipoles is that they continuously constrain ions along the magnet axis so that small misalignment between the multipole axis and magnet axis is negligible, whereas electrostatic lenses must be more accurately aligned with the magnetic field. However, multipoles limit the $m/z$ range of transmitted ions.

## 5. ORBITRAP

The orbitrap confines ions in an electrostatic quadrologarithmic potential well (37) created between carefully shaped coaxial central and outer electrodes [see **Figure 5** (38)]. Ions are pulsed into the device so that they rotate around the central electrode and oscillate along it with axial frequencies of ~50–150 kHz for $m/z$ of 200–2000. The outer electrode is split into two halves to allow differential image-current detection (39). Unlike ICR, ion excitation is not necessary to induce large amplitude, coherent oscillations, but advantages of and uses for dipolar excitation are being explored and high-resolution ion isolation has been achieved (40, 41). Instead, ions are injected with the requisite coherent motion [by use of the C-trap (42, 43)], and detection occurs immediately after all ions have been injected into the trap and after voltage on the central electrode has stabilized (44). As for the orbitrap, it is possible to detect coherent axial oscillation in a Penning (ICR) ion trap and to FT the signal to obtain a mass spectrum (45); however, because the ion cyclotron rotational frequency is typically much greater than the axial oscillation frequency in an ICR trap, cyclotron

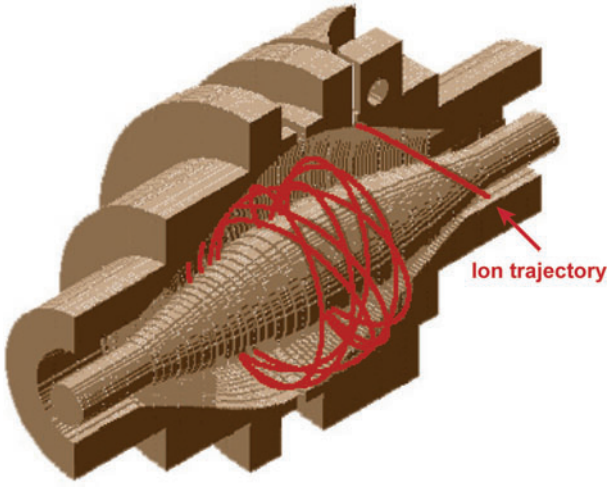


**Figure 5**

Schematic diagram of an orbitrap, showing ion injection (*upper right*) and subsequent ion trajectory. Detection is based on splitting the outer ring electrode at the trap midplane and detecting the difference in charge induced on the two halves. Figure adapted with permission from Reference 38.

rotation is preferred for detection owing to its greater frequency dispersion (and thus higher mass-resolving power).

## 5.1. Mass-Resolving Power

As for ICR frequency, the orbitrap axial oscillation frequency is independent of ion energy and amplitude and is thus ideal for $m/z$ analysis. As shown in Equation 5, the axial frequency depends only upon the ion $m/z$ and the field curvature $k$. From Equation 5, it can be shown that mass-resolving power is one-half the frequency resolving power and is proportional to $1/(m/z)^{1/2}$ (37). In this respect, the orbitrap is unlike ICR (and similar to TOF), with the consequence that mass-resolving power decreases more slowly with $m/z$ (or, conversely, improves less at lower $m/z$):

$$\nu_z = (ezk/m)^{1/2}/2\pi. \quad (5)$$

The orbitrap typically achieves a mass-resolving power of ~60,000 at $m/z$ of 400 in a 750-ms detection period. Resolving power is limited by the observation period duration, collisions with residual gas molecules, imperfections in the electric field (caused by, for example, the ion injection slot and/or inaccuracy of machining), and instability of the high-voltage power supply.

## 5.2. Mass Accuracy

Orbitrap mass inaccuracy is typically <5 ppm for externally calibrated mass spectra and <2 ppm for internally calibrated mass spectra (43). Because variability of external

calibration is dominated by instability of the inner electrode voltage, the orbitrap and its high voltage supply are thermally regulated. Internal calibration is limited by space-charge effects. However, accurate mass measurement (<5 ppm) is maintained for dynamic ranges greater than 5000 (46), which is similar to that for ICR measurements and at least an order of magnitude higher than that for TOF (47).

### 5.3. Mass Range

The mass range for a single mass spectrum may be extended by the principle of electrodynamic squeezing (37, 38). Ions are injected with several keV of kinetic energy while the voltage on the central electrode is ramped monotonically to higher amplitude so that the ion motional amplitudes shrink by a few percent during an axial oscillation period, preventing ion loss due to collisions with the outer electrode and allowing ion injection to proceed over many oscillation periods (e.g., tens of microseconds for a typical mass range of $m/z = 200$–$2000$). A further delay of some tens of milliseconds is required for voltage stabilization before image-current detection proceeds.

## 6. SELECTED APPLICATIONS

### 6.1. High Mass Accuracy: What It Can and Cannot Provide

Every isotope of every chemical element has a different mass defect (i.e., difference between exact mass and the nearest integer). Thus, sufficiently accurate mass measurement (to within ~0.0001 Da) can uniquely identify elemental composition ($C_cH_hN_nS_sO_o\ldots$). However, mass differences between isomers are too small (a difference of ~1 eV in the heat of formation corresponds to a difference of $\sim 10^{-9}$ Da) to measure in a broadband mass spectrum. The number of chemically distinct primary structures of molecules less than ~1000 Da in mass has been estimated to be greater than $10^{60}$ (48). Even if the building blocks of a molecule were known (e.g., a peptide consisting only of amino acids), more than half the pairs of peptides differing by up to three amino acids would be positional isomers (e.g., ABC versus ACB versus BCA) or substitution isomers (e.g., LeuAsn versus ValGln) (49). Thus, mass measurement cannot always yield a unique amino acid composition for a given peptide, and mass-based protein identification typically requires MS/MS (see below) to yield a sequence tag of 4–5 consecutive amino acids.

### 6.2. Need for High Mass Resolution

High mass accuracy necessarily requires resolution to yield a single mass spectral peak. For example, **Figure 6** shows MS/MS product ion spectra from a marine toxin. If only a single species were present, it would be possible to locate the center of a TOF mass spectral peak to within (say) 1/100 of the peak width, to yield a mass-measurement accuracy of a few parts per million. However, the TOF measurement in this case can never identify the analyte because the signal consists of five unresolved components.

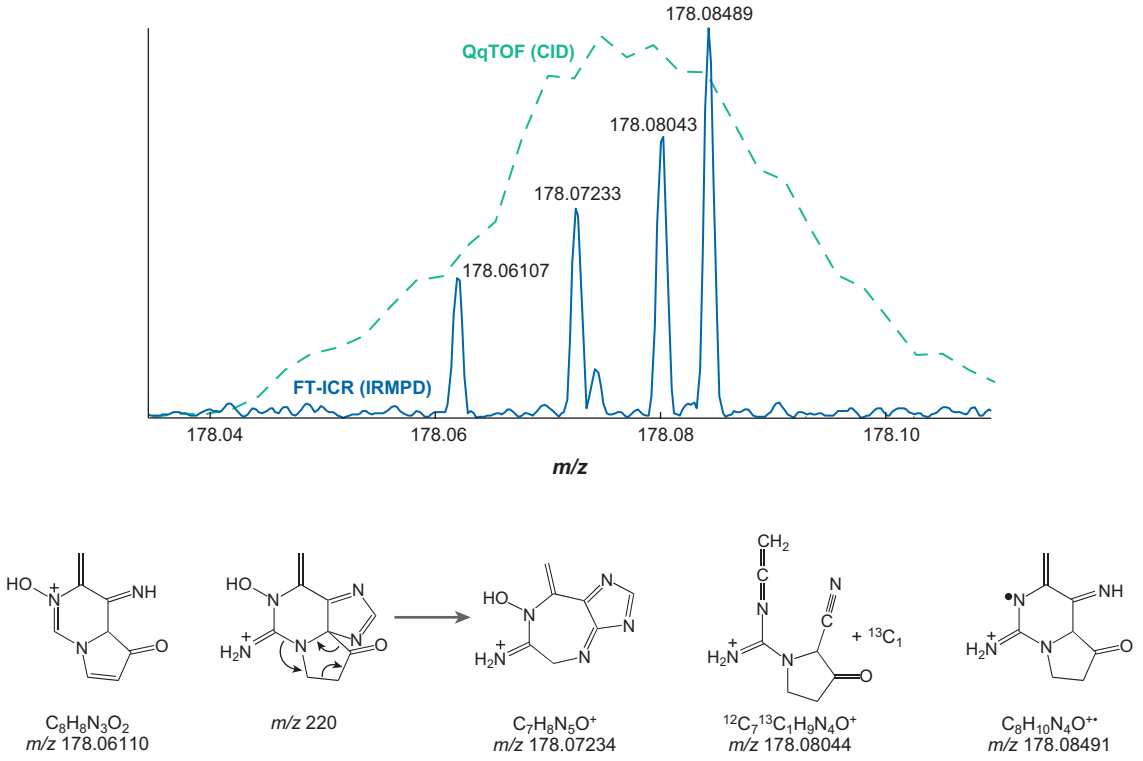


**Figure 6**

Isobaric species at *m/z* of 178 in the infrared multiphoton dissociation product ion spectrum of neosaxitoxin. The ion structures as well as their calculated exact masses are shown below the spectrum. For comparison, the quadrupole mass filters (Qq; see text) time-of-flight collision-induced dissociation (CID) spectrum is shown as a dashed line. This figure demonstrates the need for high resolution prior to mass measurement. Figure adapted with permission from Reference 72. Abbreviation: FT-ICR, Fourier transform–ion cyclotron resonance.

Thus, for any initially unknown sample, it is essential to perform high-resolution mass analysis first, to determine the number of species present.

## 6.3. Choice of Mass Analyzer

TOF mass analyzers have (in principle) no upper *m/z* limit and are thus particularly advantageous for the detection of singly charged ions greater than 5000 Da in mass (as generated by MALDI) and/or for applications requiring acquisition of more than 1 mass spectrum per second. TOF, ICR, and orbitrap mass analyzers each require a pulsed ion source: either inherently pulsed (as for MALDI) or by sudden ejection of ions accumulated continuously (as for ESI) in an external multipole ion trap. FT mass analyzers (ICR and orbitrap) are optimal for ions of $m/z < 5000$ (e.g., singly charged drugs, metabolites, and other organics and multiply charged biomacromolecules).

Relative to FT-ICR MS, the orbitrap exhibits lower mass resolution and mass accuracy, but higher sensitivity and $m/z$ range when ions are injected from an external source.

### 6.4. Tandem Mass Spectrometry

For FT-ICR, ions may be dissociated either in the ICR cell (infrared multiphoton dissociation, electron capture dissociation) or in an external electric multipole ion trap (collision-induced dissociation, CID). (CID can be conducted in the ICR cell, but subsequent high-resolution detection requires lengthy pump-down to remove the collision gas.) Advantages of in-cell dissociation include the absence of ion loss due to transmission, and TOF discrimination between the external ion trap and the ICR cell. Moreover, electron capture dissociation (see below) is optimally conducted with simultaneous or consecutive infrared heating (50). With the orbitrap, dissociation is conducted external to the orbitrap because the product ions form over a long period compared to that of an axial oscillation, and therefore are not spatially coherent for subsequent detection. Typical MS/MS modes for the orbitrap are CID and electron transfer dissociation. Orthogonal TOF mass spectrometers typically employ quadrupole mass filters (Qq) before the TOF for CID.

## 7. SELECTED APPLICATIONS

### 7.1. Proteomics

Improvements in MS instrumentation have led to tremendous growth in the field of proteomics. High resolution (to resolve overlapping isotopic distributions and identify charge state) and accurate mass measurement [to improve identification confidence and limit search space for faster data processing (51)] have led to new proteomic methodologies. Top-down proteomics analyzes intact proteins (instead of enzymatically digested peptides) to better characterize the protein state (52, 53), and has recently been coupled to on-line liquid chromatography (54). Use of accurate mass tags for digested proteins minimizes the need for time-consuming MS/MS-based peptide identification and can, in principle, improve throughput (55). Protein quantitation is also improved by accurate mass analysis (56, 57).

### 7.2. Protein Modifications

Posttranslational modifications (PTMs) play a critical role in many protein functions. High-resolution, accurate mass, and sophisticated tandem MS have combined to allow identification, localization, and characterization of a variety of biologically relevant protein modifications (58). Electron capture dissociation (59, 60) and electron transfer dissociation (61) extensively cleave peptide backbone bonds while retaining labile PTMs such as phosphorylation and glycosylation, thereby enabling PTM localization. Complementary collisional or infrared multiphoton dissociation results in extensive characterization of glycosylation (50, 62). Each MS/MS technique benefits

from high resolution and accurate mass, which are required to determine ion charge state, resolve closely spaced mass doublets, and confidently assign isobaric PTMs.

## 7.3. Metabolomics

A metabolome is the complete set of low-molecular-weight (<∼1500 Da) metabolites in an organism and varies with genotype, cell cycle stage, and environment. A recently published database of the human metabolome includes ∼2600 endogenous metabolites (and an additional 3300 drugs and food additives) (63) that vary over many orders of magnitude in concentration and require multiple ionization techniques and both mass spectrometer polarities to observe (64). Accurate mass analysis is a critical but insufficient component of metabolite identification, owing to the presence of structural isomers and the lack of elemental constraints. Chromatographic separation reduces mass spectral complexity, improves dynamic range, and can separate isomeric structures (65). Furthermore, isotopic relative abundances and probabilistic elemental constraints can reduce the number of possible elemental compositions

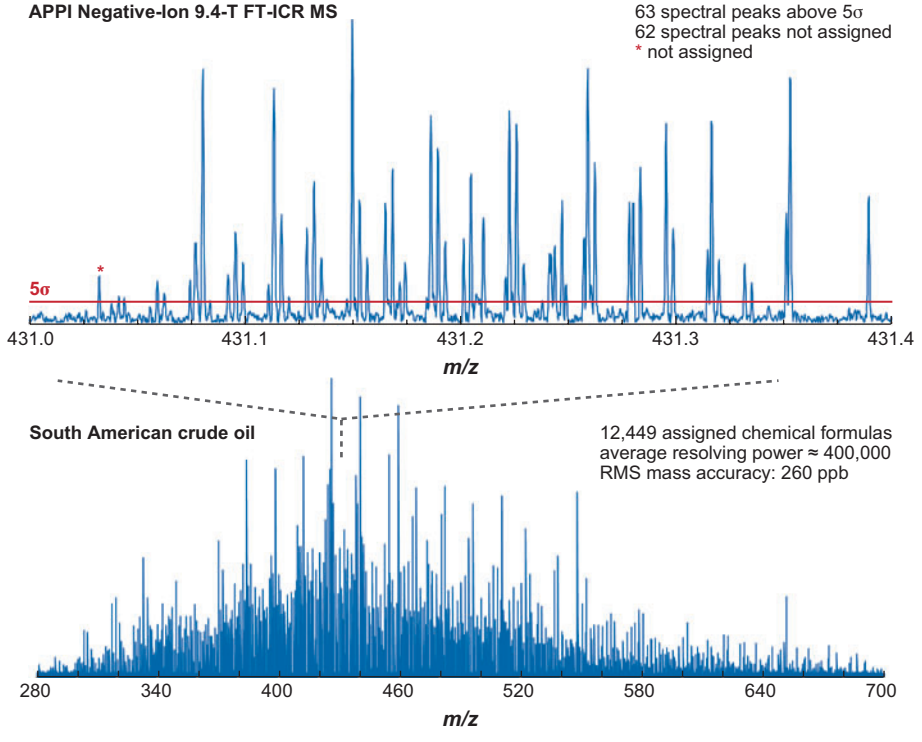


**Figure 7**

Atmospheric pressure photoionization negative ion 9.4-T Fourier transform–ion cyclotron resonance (FT-ICR) mass spectrum of a South American crude oil, showing the largest total number (and largest number spanning one Dalton) of assigned elemental compositions published to date. Figure adapted with permission from Reference 73.

(66, 67). For example, 3 ppm mass-measurement error coupled with 2% relative abundance accuracy reduces the number of possible elemental compositions below that of a mass spectrometer capable of 0.1 ppm mass error (FT-ICR MS is approaching that value).

### 7.4. Petroleomics

The most complex organic mixtures (i.e., largest number of elemental compositions within a concentration dynamic range of $\sim 10^4$:1) are derived from petroleum and its products. Ultrahigh-resolution (average $m/\Delta m_{50\%} > 300{,}000$ for $200 < m/z < 1000$) MS can resolve and identify more than 10,000 different elemental compositions in a single mass spectrum (see **Figure 7**). Such capability has spawned the new field of petroleomics (68, 69), namely, the correlation and, ultimately, prediction of the properties and behavior of petroleum and its products on the basis of knowledge of its detailed chemical composition.

#### FUTURE ISSUES

1. Much of the development of high-resolution mass analyzers to date has been guided by simulated single-ion trajectories in electric and magnetic fields. Future improvements will rely on simulations that include ion-ion Coulomb interactions as well as ion image charges on nearby electrodes.
2. Up to another twofold increase in mass-resolving power can be realized by implementation of absorption-mode rather than magnitude-mode FT spectral display (14).
3. Additional potential improvement in determination of spectral peak positions and amplitudes may become available from nonuniform time-domain sampling (the FT requires equally spaced time-domain data points) and from non-FT data reduction (14).
4. Because mass-measurement accuracy is directly proportional to mass spectral peak height-to-noise ratio (3), any improvement in ionization efficiency should translate into improved mass accuracy.

## DISCLOSURE STATEMENT

The authors are not aware of any biases that might be perceived as affecting the objectivity of this review.

## ACKNOWLEDGMENTS

This work was supported by National Science Foundation grant DMR-06-54118, Florida State University, and the National High Magnetic Field Laboratory in Tallahassee, Florida.

## LITERATURE CITED

1. Marshall AG, Hendrickson CL, Shi SD-H. 2002. Scaling MS plateaus with high-resolution FTICR MS. *Anal. Chem.* 74:252A–59A
2. Gross JH. 2004. *Mass Spectrometry: A Textbook*. Berlin: Springer. 541 pp.
3. Chen L, Cottrell CE, Marshall AG. 1986. Effect of signal-to-noise ratio and number of data points upon precision in measurement of peak amplitude, position, and width in Fourier transform spectrometry. *Chemom. Intell. Lab. Syst.* 1:51–58
4. Lee H-N, Marshall AG. 2000. Theoretical maximal precision for mass-to-charge ratio, amplitude, and width measurement in ion-counting mass analyzers. *Anal. Chem.* 72:2256–60
5. Flora JW, Harris JC, Muddiman DC. 2001. High-mass accuracy of product ions produced by SORI-CID using a dual electrospray ionization source coupled with FTICR mass spectrometry. *Anal. Chem.* 73:1247–51
6. Syka JEP, Marto JA, Bai DL, Horning S, Senko MW, et al. 2004. Novel linear quadrupole ion trap/FT mass spectrometer: performance characterization and use in the comparative analysis of histone H3 post-translational modifications. *J. Proteome Res.* 3:621–26
7. Verentchikov AN, Ens W, Standing KG. 1994. Reflecting time-of-flight mass spectrometer with an electrospray ion source and orthogonal extraction. *Anal. Chem.* 66:126–33
8. Krutchinsky AN, Chernushevich IV, Spicer VL, Ens W, Standing KG. 1998. Collisional damping interface for an electrospray ionization time-of-flight mass spectrometer. *J. Am. Soc. Mass Spectrom.* 9:569–79
9. Cotter RJ. 1997. *Time-of-Flight Mass Spectrometry: Instrumentation and Applications in Biological Research*. Washington, DC: Amer. Chem. Soc. 326 pp.
10. Mamyrin BA, Karataev VI, Shmikk DV, Zaulin VA. 1973. The mass-reflectron, a new nonmagnetic time-of-flight mass spectrometer with high resolution. *Sov. Phys. JETP* 37:45–48
11. Toyoda M, Ishihara M, Okumura D, Yamaguchi S, Katakuse I. 2001. Investigation of a multi-turn time-of-flight mass spectrometer MULTUM linear plus. *Adv. Mass Spectrom.* 15:437–39
12. Toyoda M, Okumura D, Ishihara M, Katakuse I. 2003. Multi-turn time-of-flight mass spectrometers with electrostatic sectors. *J. Mass Spectrom.* 38:1125–42
13. Satoh T, Sato T, Tamura J. 2007. Development of a high-performance MALDI-TOF mass spectrometer utilizing a spiral ion trajectory. *J. Am. Soc. Mass Spectrom.* 18:1318–23
14. Marshall AG, Verdun FR. 1990. *Fourier Transforms in NMR, Optical, and Mass Spectrometry: A User's Handbook*. Amsterdam: Elsevier. 460 pp.
15. Marshall AG, Wang T-CL, Ricca TL. 1985. Tailored excitation for Fourier transform ion cyclotron resonance mass spectrometry. *J. Amer. Chem. Soc.* 107:7893–97
16. Guan S, Marshall AG. 1993. Stored waveform inverse Fourier transform (SWIFT) axial excitation/ejection for quadrupole ion trap mass spectrometry. *Anal. Chem.* 65:1288–94

17. Comisarow MB, Marshall AG. 1974. Frequency-sweep Fourier transform ion cyclotron resonance spectroscopy. *Chem. Phys. Lett.* 26:489–90
18. Julian RK Jr, Cooks RG. 1993. Broad band excitation in the quadrupole ion trap mass spectrometer using shaped pulses with the inverse Fourier transform. *Anal. Chem.* 65:1827–33
19. Marshall AG, Comisarow MB, Parisod G. 1979. Relaxation and spectral line shape in Fourier transform ion cyclotron resonance spectroscopy. *J. Chem. Phys.* 71:4434–44
20. Bartholdi E, Ernst RR. 1973. Zero-filling analysis for FT/NMR. *J. Magn. Reson.* 11:9–19
21. Senko MW, Hendrickson CL, Emmett MR, Shi SD-H, Marshall AG. 1997. External accumulation of ions for enhanced electrospray ionization Fourier transform ion cyclotron resonance mass spectrometry. *J. Am. Soc. Mass Spectrom.* 8:970–76
22. Olsen JV, de Godoy LMF, Li G, Macek B, Mortensen P, et al. 2005. Parts per million mass accuracy on an orbitrap mass spectrometer via lock mass injection into a C-trap. *Mol. Cell. Proteomics* 4:2010–21
23. Wilcox BE, Hendrickson CL, Marshall AG. 2002. Improved ion extraction from a linear octopole ion trap: SIMION analysis and experimental demonstration. *J. Am. Soc. Mass Spectrom.* 13:1304–12
24. Comisarow MB, Marshall AG. 1974. Fourier transform ion cyclotron resonance spectroscopy. *Chem. Phys. Lett.* 25:282–83
25. Marshall AG. 2000. Milestones in Fourier transform ion cyclotron resonance mass spectrometry technique development. *Int. J. Mass Spectrom.* 200:331–36
26. Marshall AG, Hendrickson CL. 2002. Fourier transform ion cyclotron resonance detection: principles and experimental configurations. *Int. J. Mass Spectrom.* 215:59–75
27. Marshall AG, Hendrickson CL, Jackson GS. 1998. Fourier transform ion cyclotron resonance mass spectrometry: a primer. *Mass Spectrom. Rev.* 17:1–35
28. Shi SD-H, Drader JJ, Freitas MA, Hendrickson CL, Marshall AG. 2000. Comparison and interconversion of the two most common frequency-to-mass calibration functions for Fourier transform ion cyclotron resonance mass spectrometry. *Int. J. Mass Spectrom.* 195/196:591–98
29. Rainville S, Thompson JK, Pritchard DE. 2004. An ion balance for ultra-high-precision atomic mass measurements. *Science* 303:334–38
30. Guan S, Marshall AG. 1995. Ion traps for FT-ICR/MS: Principles and design of geometric and electric configurations. *Int. J. Mass Spectrom. Ion Process.* 146/147:261–96
31. Beu SC, Laude DA Jr. 1992. Open trapped ion cell geometries for FT/ICR/MS. *Int. J. Mass Spectrom. Ion Process.* 112:215–30
32. Caravatti P, Allemann M. 1991. RF shim by trap segmentation. *Org. Mass Spectrom.* 26:514–18
33. McIver RT Jr. 1990. Trajectory calculations for axial injection of ions into a magnetic field: overcoming the magnetic mirror effect with an RF quadrupole lens. *Int. J. Mass Spectrom. Ion Process.* 98:35–50

34. McIver RT Jr, Hunter RL, Bowers WD. 1985. Coupling a quadrupole mass spectrometer and a Fourier transform mass spectrometer. *Int. J. Mass Spectrom. Ion Process.* 64:67–77
35. Senko MW, Hendrickson CL, Pasa-Tolic L, Marto JA, White FM, et al. 1996. Electrospray ionization FT-ICR mass spectrometry at 9.4 tesla. *Rapid Commun. Mass Spectrom.* 10:1824–28
36. Alford JM, Williams PE, Trevor DJ, Smalley RE. 1986. Metal cluster ICR: combining supersonic metal cluster beam technology with FT-ICR. *Int. J. Mass Spectrom. Ion Process.* 72:33–51
37. Makarov A. 2000. Electrostatic axially harmonic orbital trapping: a high-performance technique of mass analysis. *Anal. Chem.* 72:1156–62
38. Hu Q, Noll RJ, Li H, Makarov A, Hardman M, Cooks RG. 2005. The orbitrap: a new mass spectrometer. *J. Mass Spectrom.* 40:430–43
39. Comisarow MB. 1978. Signal modeling for ion cyclotron resonance. *J. Chem. Phys.* 69:4097–104
40. Hu Q, Cooks RG, Noll RJ. 2007. Phase-enhanced selective ion ejection in an orbitrap mass spectrometer. *J. Am. Soc. Mass Spectrom.* 18:980–83
41. Hu Q, Makarov A, Cooks RG, Noll RJ. 2006. Resonant ac dipolar excitation for ion motion control in the orbitrap mass analyzer. *J. Phys. Chem. A* 110:2682–89
42. Kholomeev A, Makarov A, Denisov E, Lange O, Balschun W, Horning S. 2006. *Squeezing a camel through the eye of a needle: a curved linear trap for pulsed ion injection into an orbitrap analyzer*. Presented at Amer. Soc. Mass Spectrom. Conf. Mass Spectrom. & Allied Top., 54th, Seattle, Washington
43. Makarov A, Denisov E, Kholomeev A, Balschun W, Lange O, et al. 2006. Performance evaluation of a hybrid linear ion trap/orbitrap mass spectrometer. *Anal. Chem.* 78:2113–20
44. Makarov A. 2003. Interfacing the orbitrap mass analyzer to an electrospray ion source. *Anal. Chem.* 75:1699–705
45. Schweikhard L, Blundschling M, Jertz R, Kluge H-J. 1989. Fourier transform mass spectrometry without ion cyclotron resonance: direct observation of the trapping frequency of trapped ions. *Int. J. Mass Spectrom. Ion Process.* 89:R7–R12
46. Makarov A, Denisov E, Lange O, Horning S. 2006. Dynamic range of mass accuracy in LTQ orbitrap hybrid mass spectrometer. *J. Am. Soc. Mass Spectrom.* 17:977–82
47. Blom KF. 2001. Estimating the precision of exact mass measurements in an orthogonal time-of-flight mass spectrometer. *Anal. Chem.* 73:715–19
48. Hertkorn N, Ruecker C, Meringer M, Gugisch R, Frommberger M, et al. 2007. High-precision frequency measurements: indispensable tools at the core of the molecular-level analysis of complex systems. *Anal. Bioanal. Chem.* 389:1311–27
49. He F, Emmett MR, Håkansson K, Hendrickson CL, Marshall AG. 2004. Theoretical and experimental prospects for protein identification based solely on accurate mass measurement. *J. Proteome Res.* 3:61–67
50. Håkansson K, Chalmers MJ, Quinn JP, McFarland MA, Hendrickson CL, Marshall AG. 2003. Combined electron capture and infrared multiphoton dissociation for multistage MS/MS in an FT-ICR mass spectrometer. *Anal. Chem.* 75:3256–62

51. Zubarev R, Mann M. 2007. On the proper use of mass accuracy in proteomics. *Mol. Cell. Proteomics* 6:377–81
52. Kelleher NL. 2004. Top down proteomics. *Anal. Chem.* 76:196A–203A
53. Waanders MB, Olsen JV, Mann M. 2006. Top-down protein sequencing and MS3 on a hybrid linear quadrupole ion trap–orbitrap mass spectrometer. *Mol. Cell. Proteomics* 5:949–58
54. Parks BA, Jiang L, Thomas PM, Wenger CD, Roth MJ, et al. 2007. Top-down proteomics on a chromatographic time scale using linear ion trap Fourier transform hybrid mass spectrometers. *Anal. Chem.* 79:7984–91
55. Bogdanov B, Smith RD. 2005. Proteomics by FT-ICR mass spectrometry: top down and bottom up. *Mass Spectrom. Rev.* 24:168–200
56. Gruhler A, Olsen JV, Mohammed S, Mortensen P, Faergeman NJ, et al. 2005. Quantitative phosphoproteomics applied to the yeast signaling pathway. *Mol. Cell. Proteomics* 4:310–27
57. Venable JD, Wholschlegel J, McClatchey DB, Park SK, Yates JR. 2007. Relative quantification of stable isotope labeled peptides using a linear ion trap–orbitrap hybrid mass spectrometer. *Anal. Chem.* 79:3056–64
58. Meng F, Forbes AJ, Miller LM, Kelleher NL. 2005. Detection and localization of protein modifications by high-resolution tandem mass spectrometry. *Mass Spectrom. Rev.* 24:126–34
59. Cooper HJ, Håkansson K, Marshall AG. 2005. The role of electron capture dissociation in biomolecular analysis. *Mass Spectrom. Rev.* 24:201–22
60. Zubarev RA, Kelleher NL, McLafferty FW. 1998. Electron capture dissociation of multiply charged protein cations: a nonergodic process. *J. Am. Chem. Soc.* 120:3265–66
61. Syka JEP, Coon JJ, Schroeder MJ, Shabanowitz J, Hunt DF. 2004. Peptide and protein sequence analysis by electron transfer dissociation mass spectrometry. *Proc. Natl. Acad. Sci. USA* 101:9528–33
62. Håkansson K, Cooper HJ, Emmett MR, Costello CE, Marshall AG, Nilsson CL. 2001. Electron capture dissociation and infrared multiphoton dissociation MS/MS of an N-glycosylated tryptic peptide to yield complementary sequence information. *Anal. Chem.* 73:4530–36
63. Wishart DS. 2007. Proteomics and the human metabolome project. *Expert Rev. Proteomics* 4:333–35
64. Aharoni A, Ric de Vos CH, Verhoeven HA, Maliepaard CA, Kruppa G, et al. 2002. Nontargeted metabolome analysis by use of Fourier transform ion cyclotron resonance mass spectrometry. *Omics* 6:217–34
65. Ding J, Sorensen CM, Zhang Q, Jiang H, Jaitly N, et al. 2007. Capillary LC coupled with high-mass measurement accuracy mass spectrometry for metabolic profiling. *Anal. Chem.* 79:6081–93
66. Kind T, Fiehn O. 2006. Metabolomic database annotations via query of elemental compositions: mass accuracy is insufficient even at less than 1 ppm. *BMC Bioinformatics* 7:234
67. Kind T, Fiehn O. 2007. Seven golden rules for heuristic filtering of molecular formulas obtained by accurate mass spectromtry. *BMC Bioinformatics* 8:105

68. Marshall AG, Rodgers RP. 2004. Petroleomics: the next grand challenge for chemical analysis. *Acc. Chem. Res.* 37:53–59
69. Rodgers RP, Marshall AG. 2006. Chapter 3. Petroleomics: advanced characterization of petroleum-derived materials by Fourier transform ion cyclotron resonance mass spectrometry (FT-ICR MS). In *Asphaltenes, Heavy Oils, and Petroleomics*, ed. OC Mullins, EY Sheu, A Hammami, AG Marshall. New York: Springer. pp. 63–93
70. Cotter RJ. 1999. The new time-of-flight mass spectrometry. *Anal. Chem.* 71:445A–51A
71. Okamura D, Toyoda M, Ishihara M, Katakuse I. 2004. A compact sector-type multi-turn time-of-flight mass spectrometer 'MULTUM II.' *Nucl. Instrum. Methods Phys. Res. A* 519:331–37
72. Sleno L, Volmer DA, Marshall AG. 2005. Assigning product ions from complex MS/MS spectra: the importance of mass uncertainty and resolving power. *J. Am. Soc. Mass Spectrom.* 16:183–98
73. Purcell JM, Hendrickson CL, Rodgers RP, Marshall AG. 2006. Atmospheric pressure photoionization Fourier transform ion cyclotron resonance mass spectrometry for complex mixture analysis. *Anal. Chem.* 78:5906–12